Physiological limits to inshore invasion of Indo-Pacific lionfish (Pterois spp.): insights from the functional characteristics of their visual system and hypoxia tolerance

Aaron Hasenei, David W. Kerstetter, Andrij Z. Horodysky & Richard W. Brill

Biological Invasions

ISSN 1387-3547 Volume 22 Number 6

Biol Invasions (2020) 22:2079-2097 DOI 10.1007/s10530-020-02241-5



Your article is protected by copyright and all rights are held exclusively by Springer Nature Switzerland AG. This e-offprint is for personal use only and shall not be selfarchived in electronic repositories. If you wish to self-archive your article, please use the accepted manuscript version for posting on your own website. You may further deposit the accepted manuscript version in any repository, provided it is only made publicly available 12 months after official publication or later and provided acknowledgement is given to the original source of publication and a link is inserted to the published article on Springer's website. The link must be accompanied by the following text: "The final publication is available at link.springer.com".



Check for updates

ORIGINAL PAPER

Physiological limits to inshore invasion of Indo-Pacific lionfish (*Pterois* spp.): insights from the functional characteristics of their visual system and hypoxia tolerance

Aaron Hasenei · David W. Kerstetter · Andrij Z. Horodysky · Richard W. Brill

Received: 14 February 2019/Accepted: 10 March 2020/Published online: 16 March 2020 © Springer Nature Switzerland AG 2020

Abstract Indo-Pacific lionfish (*Pterois* spp.) have become established throughout the Caribbean and the coastal regions of the Gulf of Mexico and western Atlantic Ocean from North Carolina to central Brazil. Lionfish may also invade estuaries, as they tolerate salinities down to 4‰. We hypothesize that the functional characteristics of their visual system (which evolved in the clear tropical waters of the Indo-Pacific) or their inability to tolerate hypoxia will limit the capacity of lionfish to occupy these areas. We assessed the former with corneal electroretinography and the latter with intermittent-flow respirometry. The luminous sensitivity, temporal resolution (quantified as flicker fusion frequency), and spectral sensitivity of the lionfish visual system are like those of native piscivores, indicating that their visual system will be functional under estuarine photic conditions and allow lionfish to be effective piscivores. In contrast, acute

exposure to reduced oxygen levels (equivalent to those commonly occurring in mid-Atlantic and Gulf of Mexico estuaries) exceeded the physiological tolerances of lionfish. We therefore conclude that hypoxia will control or limit estuarine invasion.

Keywords Invasion · Estuaries · Ecophysiology · Vision · Scope for activity

Introduction

Since their introduction in Florida in 1986 from the aquarium trade, Indo-Pacific lionfish (Pterois spp.) have become established throughout the Caribbean as well as the coastal regions of the Gulf of Mexico and western Atlantic Ocean (from North Carolina to central Brazil) (Courtenay 1995; Semmens et al. 2004; González et al. 2009; Whitfield et al. 2014; Ferreira et al. 2015; Hixon et al. 2016). Multiple factors (e.g., lack of natural predators, lionfish's high fecundity, naivety of native prey species, etc.) have enabled rapid range expansion (Fishelson 1997; Whitfield et al. 2002; Côté et al. 2013; Green et al. 2011, 2019; Morris 2012; Albins and Hixon 2013; McCormick and Allan 2016). Lionfish can reduce native fish recruitment on coral reefs by up to 79%, locally extirpate native species, and (at densities reported in the Caribbean) potential remove approximately > 900 kg of prey per hectare of reef habitat

A. Hasenei · D. W. Kerstetter Department of Marine and Environmental Sciences, Halmos College of Natural Sciences and Oceanography, Nova Southeastern University, Fort Lauderdale, FL 33004, USA

A. Z. Horodysky Department of Marine and Environmental Science, Hampton University, Hampton, VA 23668, USA

R. W. Brill (

Department of Fisheries Science, Virginia Institute of Marine Science, Gloucester Point, VA 23062, USA e-mail: rbrill@vims.edu



per year (Whitfield et al. 2002; Albins and Hixon 2008; Côté and Maljković 2010; Green et al. 2012; Cerino et al. 2013; Ingeman 2016). For these reasons, lionfish are a significant threat to native fish populations and local biodiversity (Côté and Smith 2018).

Because estuaries are important nursery habitats for many commercially, recreationally, and ecologically important fish species (Beck et al. 2001; Courrat et al. 2009), we contend that it is critical to understand the ability of lionfish to occupy these inshore areas. Although lionfish commonly associate with tropical and sub-tropical coral reefs in the Indo-Pacific, in the western Atlantic they are found in mangrove systems and seagrass meadows, and around artificial structures; indicating their behavioral adaptability (Barbour et al. 2010; Jud et al. 2011). Lionfish can tolerate salinities as low as 4% ($\approx 10\%$ seawater) and have already become established in the Loxahatchee River estuary (on the Atlantic coast of Florida, USA) (Jud et al. 2011, 2014). Lionfish are also more eurythermal (tolerance range $\approx 10-39$ °C) than other tropical species and can survive temperatures as low as ≈ 10–12 °C with gradual acclimation (Dabruzzi et al. 2017; Barker et al. 2017). Low winter temperatures are likely to be ineffective at preventing permanent establishment in estuaries that remain above 10 °C (Baumann and Smith 2018). With ongoing increases in ocean temperature due to directional climate change, lionfish are also likely to distribute to higher latitudes (Côté and Green 2012; Whitfield et al. 2014; Sandblom et al. 2014; Bernal et al. 2015). In brief, lionfish appear to be equipped physiologically to invade estuaries throughout the Gulf of Mexico, the U.S. South Atlantic Bight (i.e., Florida through North Carolina), and farther north at least seasonally.

We hypothesize, however, that the unique visual environment (Lythgoe 1979, 1988) and episodic hypoxia (lasting minutes to days) common in estuaries (Breitburg 1992; Rabalais et al. 2010; Baumann and Smith 2018) could limit the ability of lionfish to invade these ecologically critical areas. To test our hypothesis, we employed standard physiological techniques to investigate:

- 1. the functional characteristics of the lionfish visual system,
- 2. the effects of temperature and hypoxia on standard metabolic rate (SMR, the minimum metabolic rate

- of a fasting, resting animal), active metabolic rate (AMR, the metabolic rate elicited from exhaustive exercise); and scope for activity (the difference between AMR and SMR),
- 3. the minimum survivable oxygen levels at different temperatures.

We took this approach because we contend (as have others, e.g. Browman 2005; Cooke and Suski 2008; Dangles et al. 2009; Cooke and O'Connor 2010; Cooke et al. 2013; Horodysky et al. 2015; McKenzie et al. 2016) that physiological data can provide mechanistic insights into drivers of fish behavior, distribution, and ecology to the benefit of fisheries and ecosystem management. This includes the management of invasive species (Lennox et al. 2015).

Maintaining optimal visual performance in estuaries is challenging because they are some of the most photodynamic habitats on earth (Lythgoe 1979, 1988; Loew and McFarland 1990). This arises from seasonal changes in stratification and mixing, wave action, weather, solar irradiance, phytoplankton abundance, and anthropogenically induced processes such as eutrophication and sedimentation (McFarland and Loew 1983; Wing et al. 1993; Schubert et al. 2001; Gallegos et al. 2005; Kemp et al. 2005). Because the visual systems of fishes reflect the characteristics of the light fields they inhabit (Munz and McFarland 1973; Muntz 1990; Guthrie and Muntz 1993), and because lionfish evolved in the clear waters of the tropical Indo-Pacific, we hypothesize they will face challenges with respect to effective prey detection and capture in estuarine environments. To test this hypothesis, we determined the functional characteristics of their visual system using corneal electroretinography. The recorded electroretinogram (ERG) is the summed potentials of various cell types within the retina produced in response to light stimuli (Brown 1968; Ali and Muntz 1975). Electroretinography is thus wellsuited for investigation of the functional properties of the visual system. More importantly, we were able to compare our data to data on the functional characteristics of visual systems of four native piscivores common in western mid-Atlantic estuaries collected using identical procedures (Horodysky et al. 2010).

Significant information exists on visual function in fishes (e.g., Douglas and Djamgoz 1990; Ladich et al. 2006), but we know of only one study on the visual function in lionfish which dealt primarily with the



effects of prolonged exposure to monochromatic light on spectral sensitivity (Carroll 2018). We quantified three visual parameters considered fundamental predictors of teleost light niches and feeding ecologies (Lythgoe 1979; Muntz 1990; Horodysky et al. 2008, 2010, 2013): luminous sensitivity, flicker fusion frequency (FFF), and spectral sensitivity. Luminous sensitivity includes two metrics: K_{50} (a measure of light sensitivity) and dynamic range (i.e., the range of detectable light levels). FFF is a measure of temporal resolution and spectral sensitivity is a measure of the range of perceivable wavelengths (i.e., colors). The latter also allows inference of the number of visual pigments present and their relative abundance.

The effects of temperature and hypoxia controlling or limiting the distribution of invasive fish species has received considerable attention (e.g., Kimball et al. 2004; Whitfield et al. 2014; Marras et al. 2015; Barker et al. 2017), but whether the interactive effects of temperature and hypoxia could limit the inshore invasion of lionfish remains unclear. We therefore measured the effects of temperature and hypoxia on SMR, AMR, and scope for activity; the latter being the total amount of energy apportioned between growth, reproduction, movement, and the maintenance of homeostasis. Temperature and hypoxia influence SMR, AMR, maximum metabolic rate (MMR), and scope for activity as they shape the ability of the cardiorespiratory system to deliver oxygen and metabolic substrates tissues to the 1947, 1971; Fry and Hart 1948; Clark et al. 2013; Horodysky et al. 2015; Norin and Clark 2016; Pörtner et al. 2017). The high spatial and temporal variability of temperature and dissolved oxygen levels in estuaries is well documented (e.g., Breitburg 1992; Breitburg et al. 2003; Diaz 2001; Diaz and Breitburg 2009; Rabalais et al. 2010; Baumann and Smith 2018). Episodic hypoxia (lasting minutes to days) occurs during the summer and early autumn when decomposition of organic matter consumes dissolved oxygen and density-driven stratification prevents oxygen-rich surface water from mixing with hypoxic bottom water (Bishop et al. 2006; Tyler et al. 2009). Measurement of the effects of temperature and hypoxia on SMR, AMR, and scope for activity therefore allows insight as to whether lionfish have the physiological abilities to invade estuaries.

Methods

All husbandry and experimental procedures were approved by the Institutional Animal Care and Use Committees of Nova Southeastern University (protocol number 2017-DK2) and the College of William and Mary (protocol number IACUC-2018-01-16-12610-rwbril). Lionfish (80–250 mm total length, 38-140 g) were collected in the Florida Keys and held at the Guy Harvey Oceanographic Center, Nova Southeastern University (Dania Beach, FL, USA) for a minimum of 2 weeks before use in experiments. Fish were maintained in recirculating aquaria at 25 \pm 2 °C and 20 \pm 2‰ to approximate summertime estuarine conditions. Indirect illumination was provided by sunlight transmitted through the windows of the holding facility. Fish were fed a mixture of live grass shrimp (Palaemonetes paludosus), commercially available frozen bay scallops, shrimp, and sardines ad libitum three times per week. After the acclimation period, a subset of fifteen subjects were transported to the Virginia Institute of Marine Science (Gloucester Point, VA, USA) for experiments on visual function.

Electroretinography

Subjects were removed from the holding tanks during daylight hours, sedated with ketamine hydrochloride (30 mg kg⁻¹), and immobilized with the neuromuscular blocking drug gallamine triethiodide (10 mg kg⁻¹); both delivered intramuscularly. Fish were then transferred to a light-tight experimental enclosure and placed on a cloth sling within a rectangular Plexiglas tank so that only a minimal portion of the head and one eye remained above the water. Subjects were ventilated with temperaturecontrolled (25 \pm 2 °C) aerated water (salinity 20‰) to minimize any confounding effects of temperature (Saszik and Bilotta 1999; Fritsches et al. 2005), and dark adapted for a minimum of 60 min. Lionfish are crepuscular in their native range, but active during daylight hours on Bahamian coral reefs (Green et al. 2011; Côté and Maljković 2010). We therefore conducted experiments exclusively during daylight hours. Recording of the ERG of anaesthetized and immobile subjects is a common practice to minimize the obscuring effects of overt movements (e.g., Parkyn and Hawryshyn 2000; Horodysky et al. 2008). Because fish do not recover muscular movements



under these circumstances, individuals were immediately euthanized at the end of an experiment with an overdose of sodium pentobarbital (350 mg kg⁻¹ or $\approx 10 \times$ the anesthetic dose).

We used Teflon®-coated silver-silver chloride wire electrodes to record the ERG by placing the active electrode on the corneal surface and the reference electrode in the incurrent nares. Signals were amplified with a DAM50 amplifier (World Precision Instruments, Sarasota, FL, USA) using a 10,000x gain, with 1 Hz high pass and 1 k Hz low pass filters. The amplified signal was further filtered with a HumBug active electronic filter (Quest Scientific, North Vancouver, BC, Canada) to remove 60 Hz noise, and digitized at a 1 kHz sampling frequency with a multifunction data acquisition card (model 6024E, National Instruments, Austin, TX, USA). Stimuli were controlled, and the ERG recorded, using custom software (originally developed by Eric Warrant and colleagues, University of Lund, Sweden) running under Labview 2010 (National Instruments).

To assess luminous sensitivity, we presented logarithmically increasing white light stimuli to generate an intensity-response curve ("V log I curve"), where "V" refers to the amplitude of the b-wave of the ERG and "I" light intensity as described by Horodysky et al. (2008) and Kalinoski et al. (2014). A custombuilt single LED light source (working range approximately $1-1 \times 10^4$ cd m⁻²), with an attached diffuser and collimating lens, produced an even illumination field. The light source was positioned ≈ 5 cm from the cornea, such that the entire eye was exposed to light stimuli. The analog output of the multifunction data acquisition card controlled the absolute brightness of the lamp and we used combinations of 1 and 2 log unit neutral density filters (Kodak Optical Products, Rochester, NY, USA) to further adjust the range of light intensities. We calibrated the relationship of voltage input to the lamp and absolute light intensities using a research-grade radiometer (model IL1700 International Light, Peabody, MA, USA).

Stimuli progressed from subthreshold to saturation intensity (i.e., when the amplitude of ERG b-wave began to decrease in response to increases in light intensity) in 0.2-log unit steps. A train of 200 ms flashes was presented at each intensity step, and the b-wave amplitude in response to the last light flash recorded. Each train of light flashes (at a given intensity) was repeated five times, separated by a five

second rest period, and responses averaged. The sequence of light stimuli was then repeated at the next intensity step. We subsequently normalized the data to the maximum voltage response (V_{max}) for each individual, such that $V_{max} = 100\%$. The normalized data for each fish were subsequently averaged and the resultant V log I data again normalized such that mean $V_{max} = 100\%$. The log light intensity and normalized data for each fish were also fit to a 6-degree polynomial equation and the light intensity needed to produce response 5%, 50% and 95% of V_{max} for each fish determined from the predicted normalized response data. We quantified luminous sensitivity (K_{50}) as the light intensity eliciting a response 50% of V_{max} and dynamic range as the difference in irradiances needed to produce responses 5 and 95% of V_{max}. These procedures are commonly used to characterize the luminous sensitivity and operational range of the visual system (Frank 2003; Horodysky et al. 2008, 2010; Brill et al. 2008; Kalinoski et al. 2014).

We determined flicker fusion frequency (FFF) to quantify retinal temporal resolution (i.e., the ability of the retina to follow a white light source modulated at logarithmically increasing frequencies). We employed the LED system used in the intensity-response experiments to produce sinusoidally-modulated white light stimuli ranging in frequency from 1 Hz (0 log units) to 100 Hz (2.0 log units) in increments 0.2 log unit frequency steps. Each train of light flashes (at a given frequency) was repeated five times separated by 5 s of darkness and the responses averaged. To determine a subject's FFF at a given light intensity, we subjected the power spectrum of the averaged ERG data to spectral analysis and compared the power of the predominant frequency (signal) to the power of a neighboring range of higher frequencies (noise). FFF was taken as the frequency at which the power of the signal fell below a level that was five times the power of the noise. We conducted FFF experiments at light intensities (based on V log I curves) necessary to produce a maximal response and a response 25% of maximum (I_{max} and I₂₅, respectively) and assumed the former to be the maximum FFF attainable and the latter to approximate FFF at ambient light intensity.

We assessed spectral sensitivity using methods described in Horodysky et al. (2008, 2010). The output of a xenon light source (ILC Technology, Sunnydale, California, USA; calibrated in 10 nm steps using the radiometer system described above) was passed



through two AB301 filter wheels containing quartz neutral density filters (CVI Laser Spectral Products, Albuquerque, NM, USA) via a one-centimeter diameter light guide. The first wheel allowed light attenuation from 0 to 4 log units in 1 log unit steps and the second in 0–1 log units of light intensity in 0.2 log unit steps (i.e., the two wheels allowed attenuation 0–5 log units in 0.2 log unit steps). A lens focused the attenuated light beam onto the entrance slit of a monochromator (CVI Laser Spectral Products) to produce monochromatic light (50% width = 5 nm). We positioned the exit aperture of second one-centimeter diameter light guide (conducting light stimuli from the exit port of the monochromator) ≈ 5 cm from the cornea. The output of the lamp was selectively attenuated by the neutral density filters to produce approximately iso-quantal light stimuli presented in sequential 10 nm steps from 300 nm (ultraviolet, UV) to 700 nm (the longest wavelength in the human visual spectrum). Stimulus flash duration (40 ms) was controlled by a Uniblitz LS6 electronic shutter (Vincent Associates, Rochester, NY, USA) triggered by the Labview program. We presented subjects with five stimulus flashes at each wavelength, each followed by 5 s of darkness, and b-wave amplitudes at each wavelength were averaged to produce raw spectral response curves.

Spectral V log I curves (from five to zero log unit light intensity attenuation in 0.2 log unit steps) were then determined at the wavelength producing the maximal response using five (40 ms duration) stimulus flashes, each followed by 5 s of darkness. We averaged the data from responses at each light intensity to fit the resultant V log I curve to a six-degree polynomial. The inverse of this curve (i.e., swapping the dependent and independent variables) was created by extrapolation. The stimulus intensities at each wavelength were then converted to isoquantal intensities (I) and the raw spectral response curves transformed to sensitivities (S) through the equation:

$$S = 100 \times 10^{(I_{max} - I_N)} \tag{1}$$

where I_{max} is light intensity producing the maximum b-wave amplitude, and I_N the intensity needed to produce a given b-wave amplitude (Coates et al. 2006). For each fish, sensitivity at each wavelength step was expressed as a percentage of the maximal response (i.e., 100% = maximum sensitivity). The

normalized data for each fish were subsequently averaged and the resultant spectral sensitivity data again normalized such that $V_{max} = 100\%$.

To assess the wavelengths passed by the lionfish visual system, we harvested the eye lenses, corneas, and vitreous humor from three euthanized subjects and positioned them in UV transmitting cuvettes (filled 0.9% saline solution). Cuvettes were placed in a spectrophotometer (BioSpec-1601 Shimadzu Scientific Instruments, Columbia, MD, USA) and percent transmittance data recorded over 300–700 nm wavelengths in 0.5 nm steps.

Data analysis: electroretinography

Data on the functional properties of the visual systems of four estuarine piscivores (Horodysky et al. 2010; permission for use was granted by the authors and the *Journal of Experimental Biology*) were used for comparisons to those of the lionfish visual system: striped bass (*Morone saxatilis*), bluefish (*Pomatomus saltatrix*), cobia (*Rachycentron canadum*), and summer flounder (*Paralichthys dentatus*). Our procedure thus allowed direct comparisons where data were collected using the same equipment, calibration standards, experimental methods, and data analysis procedures.

We used a one-way ANOVA with pairwise multiple comparison procedure (SigmaPlot 11.0, Systat Software, San Jose, CA, USA) to compare dynamic range, K_{50} , and FFF values of lionfish to those of the estuarine piscivores. Data met assumptions of normality and homogeneity of variance and p-values less than 0.05 were taken as the fiducial level of significance.

To determine the potential number and relative abundance of visual pigments present in lionfish retina, we generated multiple hypotheses by fitting SSH (Stavenga et al. 1993) and GFRKD (Govardovskii et al. 2000) al rhodopsin absorption templates separately to the spectral sensitivity data (as described by Horodysky et al. 2008, 2010). The best fitting model parameters were objectively chosen using Akaike's information criterion (AIC) for maximum likelihood.



Respirometry

To approximate the temperatures lionfish could encounter in western Atlantic and Gulf of Mexico estuaries (Kimball et al. 2004; Baumann and Smith 2018), we conducted experiments at 15 °C, 20 °C, 25 °C, and 30 °C. Fish were acclimated for a minimum of 2 weeks at these test temperatures and fasted for 48 h prior to use in an experiment.

We determined metabolic rates using intermittent-flow respirometry, a standard procedure for estimating SMR, AMR, and hypoxia tolerances (e.g., Horodysky et al. 2011; Lapointe et al. 2014; Chabot et al. 2016; Rogers et al. 2016; Svendsen et al. 2016; Snyder et al. 2016). To determine hypoxia tolerance, we measured the critical oxygen level, which is defined as the ambient oxygen level below which an individual can no longer maintain a stable rate of oxygen consumption (e.g., Claireaux and Chabot 2016). We note, however, that the utility of this technique has been both questioned (Wood 2018) and considered appropriate for comparative studies (Ultsch and Regan 2019).

Our intermittent-flow respirometry system encompassed a cylindrical 4.6-liter plexiglass respirometry chamber (Loligo Systems, Viborg, Denmark) and fiber optic oxygen sensor and oxygen meter (PyroScience, Aachen, Germany). The entire system controlled by a computer running AquaResp2 (DTU-Aqua; http:// www.aquaresp.com/). Oxygen saturation (%) data were converted to oxygen content (mg $O_2 l^{-1}$) using standard equations (Richards 1965; Steffensen 1989) within the AquaResp2 software routines. During experiments to measure hypoxia tolerance, oxygen levels were regulated by bubbling nitrogen into the outer water bath. The respirometer was covered with black plastic to minimize visual disturbance. Metabolic rate (MO₂) measurements were made over cycles consisting of a 5-min flush period and 2-min equilibration interval, followed by a measurement interval chosen to allow oxygen levels within the respirometer to be reduced by approximately 10%. After the data recording interval, the AquaResp2 software executed a linear regression of oxygen concentration (mg 1^{-1}) against measurement time to determine the slope of this relationship (α , in mg $O_2 l^{-1} h^{-1}$). MO_2 (mg O₂ kg⁻¹ h⁻¹) values during each measurement cycle were calculated as:



where $V_{\rm rem}$ is the respirometer volume minus the fish volume (assuming 1 g of fish mass = 1 ml) and $m_{\rm f}$ is the mass of the fish in kg. We determined background oxygen consumption by measuring the rate of decline in oxygen within the respirometer when a fish was not present. We subtracted this value from all the α values when an individual was in the respirometer.

Fish were placed in the respirometer for 24 h and SMR in normoxia was determined by calculating the average of the ten lowest MO2 values (as recommended by Chabot et al. 2016). Critical oxygen levels (S_{crit}, expressed in percent air saturation) were subsequently determined by decreasing the oxygen level in the respirometer in a step-wise fashion until the metabolic rate declined in unison with further reductions in ambient oxygen. Up to four MO₂ measurements were taken at each of nine different oxygen levels (90, 80, 70, 60, 50, 40, 30, 20, and 10% of air saturation). Individual S_{crit} values were calculated using a two-piece segmented regression (SegReg; https://www.waterlog.info/segreg.htm). S_{crit} trials took approximately 8-12 h. We then left individuals undisturbed in the respirometer at full oxygen saturation until the next day.

To measure active metabolic rate (AMR), we removed individuals from the respirometer and placed them in a tank where they were gently chased to induce burst swimming to the point of exhaustion (determined by when an individual would no longer respond to prodding and remained motionless after being removed from the water). Fish were then weighed and immediately transferred to the respirometer where MO₂ was measured continuously for 48 h. AMR was calculated as the mean of the highest ten MO₂ measured over the first 12 h. We then allowed individuals a minimum 1-week recovery period before we subjected them to the protocol described above, but where metabolic rate measurements were made at ambient oxygen levels 15-20% greater than the subject's S_{crit}. We calculated AMR under hypoxia as described above, and aerobic scope values (under normoxia and hypoxia) as the differences between SMR and AMR.



Data analysis: respirometry

We used a one-way repeated measures ANOVA with pairwise multiple comparison procedure (SigmaPlot 11.0, Systat Software) to analyze the effects of temperature and hypoxia on SMR, AMR, scope for activity, and relative scope for activity, as well as the same procedure to analyze the effects of temperature on S_{crit}. Data met assumptions of normality and homogeneity of variance and p-values less than 0.05 were taken as the fiducial level of significance. Where increases in temperature had a significant effect on SMR or AMR, we also calculated Q₁₀ values (i.e., the relative change per 10 °C change in temperature) following Prosser (1973):

$$Q_{10} = (K_1/K_2)^{10/(t_1 - t_2)} \tag{3}$$

where $K_1 = SMR$ or AMR at temperature t_1 and $K_2 = SMR$ or AMR at temperature t_2 .

Results

Visual function

Amplitude of the b-wave increased with stimulus intensity reaching maximum amplitude (V_{max}) at 1.6 ± 0.1 log light intensity, then declined presumably due to photoreceptor saturation (Fig. 1). The median K_{50} of lionfish is significantly below that of striped bass, bluefish and cobia, but not different from

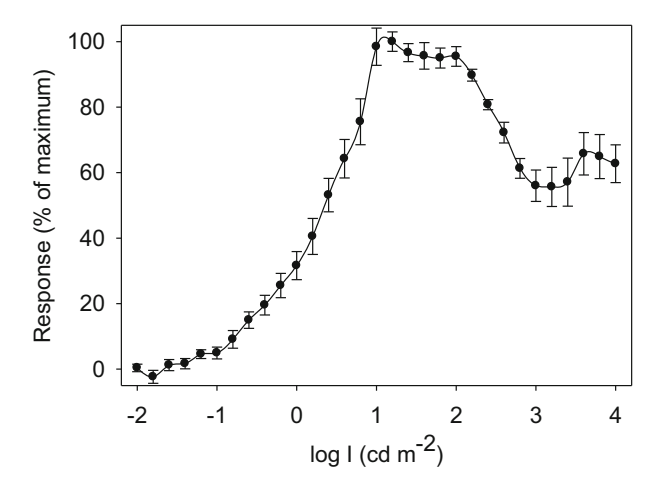


Fig. 1 Luminous sensitivity based on response—intensity (i.e., V log I) curves of lionfish. Data points are means (\pm SEM). Response values for individuals were normalized to 0–100%, the values averaged, and the mean values rescaled to 0–100%

that summer flounder (Fig. 2). Based on units of absolute light intensity (i.e., candela m $^{-2}$), lionfish are approximately 36, 4, and 5 times more light sensitive than striped bass, bluefish and cobia, respectively. In contrast, the median dynamic range of lionfish is not significantly different than that of other estuarine fishes, except for summer flounder (Fig. 2). Based on units of absolute light intensity (i.e., candela m $^{-2}$), the dynamic range of lionfish is $\approx 30\%$ that of summer flounder.

Median FFF responses for lionfish were 35 and 88 Hz at I_{25} and I_{max} , respectively (Fig. 3). At I_{25} , the median FFF lionfish is not different from any of the four other estuarine piscivores (Fig. 3). At I_{max} , however, median FFF lionfish is 41%, 36%, and 26% higher than those of summer flounder, bluefish, and cobia, respectively.

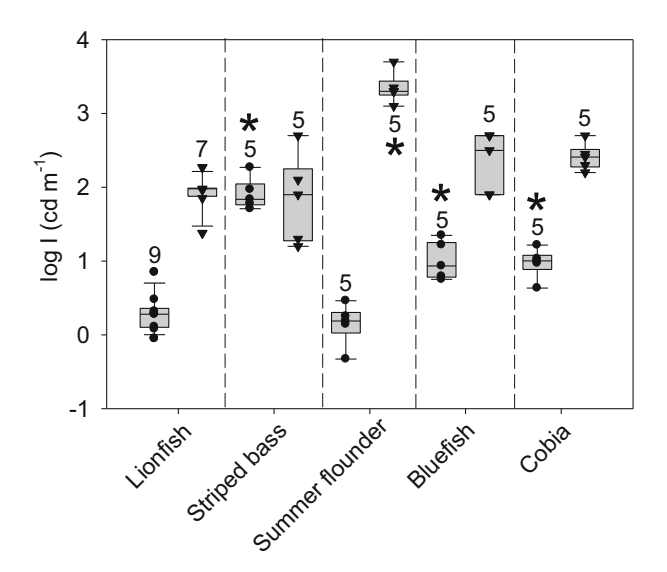


Fig. 2 Interspecific comparisons of the K_{50} (circles) and dynamic range (triangles) lionfish versus those of native estuarine piscivores (data for the latter are from Horodysky et al. 2008, 2010; consent to use these data was granted by the Journal of Experimental Biology). The "*" symbol indicates significant differences from values for lionfish and numerical values signify the number of individuals tested. Here, and in subsequent figures, we present our data as box-and-whisker plots with the individual data points shown to allow comparison of the distributions and scatter (as recommended by Weissgerber et al. 2015). The boundary of the box closest to zero indicates the 25th percentile, the line within the box marks the median, and the boundary of the box farthest from zero indicates the 75th percentile. Whiskers (error bars) above and below the box indicate the 90th and 10th percentiles, respectively. Data points above and below the 90th and 10th percentiles are considered outliers



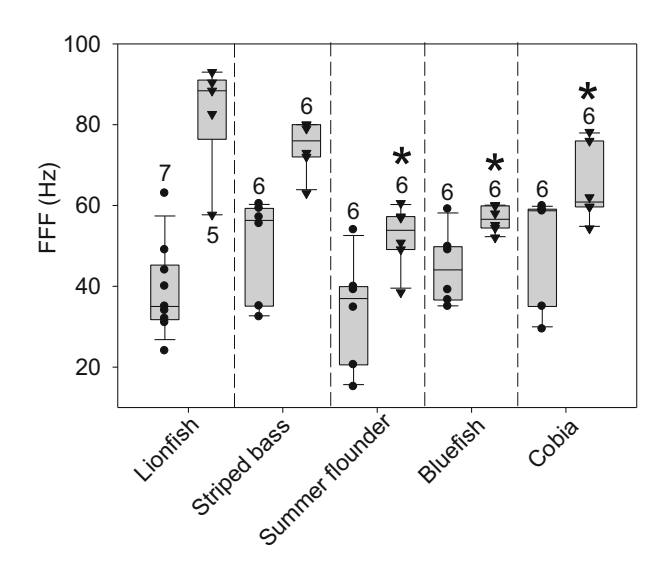


Fig. 3 Flicker fusion frequencies (FFF) values of lionfish at light intensities needed to produce a response of 25% of V_{max} (circles) and 100% of V_{max} (triangles) versus those of native estuarine piscivores (data for the latter are from Horodysky et al. 2008, 2010; consent to use these data was granted by the authors and the *Journal of Experimental Biology*). The "*" symbol indicates significant differences from values for lionfish and numerical values signify the number of individuals tested. The boundary of the box closest to zero indicates the 25th percentile, the line within the box marks the median, and the boundary of the box farthest from zero indicates the 75th percentile. Whiskers (error bars) above and below the box indicate the 90th and 10th percentiles, respectively. Data points above and below the 90th and 10th percentiles are considered outliers

Spectral sensitivity lionfish of spanned 350–630 nm with peak sensitivity 510 nm (Fig. 4). The maximum likelihood estimation using published rhodopsin templates (Govardovskii et al. 2000 and Stavenga et al. 1993; GFRKD and SSH, respectively) suggest that lionfish have three visual pigments (Table 1). The spectral sensitivity curve was optimally fitted with both SSH and GFRKD templates (i.e., the fits were statistically indistinguishable because the AIC was less than 5, Table 1). Both rhodopsin templates predicted the presence of a short wavelength ($\lambda_{\text{max}} = 381-384 \text{ nm}$), an intermediate wavelength ($\lambda_{\text{max}} = 434-443 \text{ nm}$), and a long wave pigment ($\lambda_{\text{max}} = 512-513 \text{ nm}$) (Table 1); with the long wavelength pigment being predominant (Fig. 4).

Lionfish lens and cornea displayed 80% transmittance (Fig. 5) at the peak absorbance–wavelength ($\lambda_{max} = 512-513$ nm) of the predominate retinal pigment, and 50% transmittance at the peak absorbance–wavelength ($\lambda_{max} = 381-384$ nm) of the retinal pigment responsive to shortest wavelength (Fig. 4). The

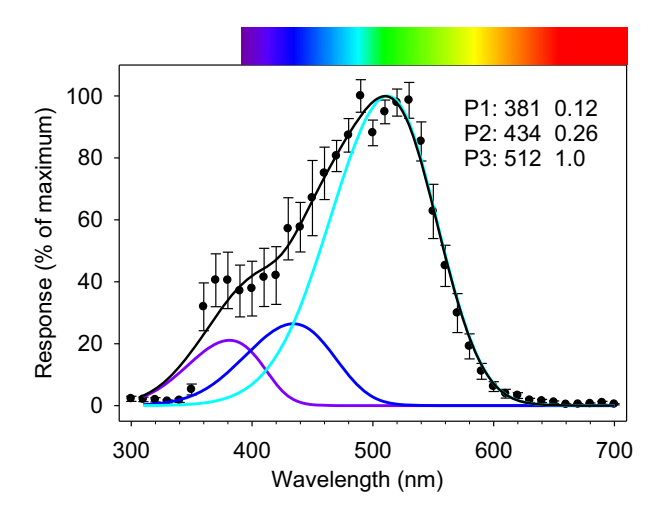


Fig. 4 Spectral sensitivity of lionfish. Data points (filled circles) are means (\pm SEM). Response values for individuals were normalized to 0–100%, the values averaged, and the mean values rescaled to 0–100%. The color-coded lines (showing the absorptive characteristics of individual visual pigments) are based on the best fitting rhodopsin template (Table 1). Wavelengths at maximal absorption of the short, medium, and longwave pigments (P1, P2, and P3, respectively in nm) and pigment-specific weighting values are shown. The black line shows the summed values of the visual pigment curves multiplied by their respective weighting factors. The color bar indicates the approximate human visible spectrum

cornea and lens also had significant transmittance of UV wavelengths (i.e., below 360 nm).

SMR, AMR, and scope for activity

The SMR of lionfish increased with temperature, except between 15 and 20 °C (Fig. 6). Q₁₀ values (based on median SMR data) were 3.8 and 4.0 between 20-25 °C and 25-30 °C (respectively). Translated into fractional increases of SMR, these are 196 and 199%, respectively. Increases in temperature elevated the AMR of lionfish, except between 15 and 20 °C (Fig. 6). Q₁₀ values (based on median AMR data) were 2.6 and 1.7 between 20-25 °C and 25-30 °C (respectively). Translated into fractional increases of AMR, these are 160 and 131%, respectively. Hypoxia reduced median AMR only at 20 °C and 25 °C; by 43 and 87 mg O₂ kg⁻¹ h⁻¹ in absolute terms and by 47 and 11% in relative terms, respectively (Fig. 6). In normoxia, median scope for activity increased only between 20 and 25 °C with a Q₁₀ value of 2.2; which is 155% increase. In hypoxia, median scope for activity increased only between 25 and 30 °C with a Q₁₀ value of 3.1; which is 176% increase (Figure 7). More



Table 1 Rhodopsin templates (based on Govardovskii et al. 2000 and Stavenga et al. 1993; GFRKD and SSH, respectively) fitted to
ERG data

Condition	Template	$\lambda_{max,1}$	$\lambda_{max,1}$	$\lambda_{\text{max},1}$	p	AIC	ΔΑΙС
Mono	SSH	505			2	- 90	96
	GFRD	504			2	- 104	82
Di, α	SSH	411	510		5	- 172	14
	GFRD	410	510		5	- 173	13
Di, β, S	SSH	460	513		6	- 181	5
	GFRD	411	510		6	- 170	16
Di, β, L	SSH	461	513		6	- 181	5
	GFRD	439	513		5	- 147	39
Di, β, B	SSH	498	520		6	- 177	9
	GFRD	437	512		6	- 130	56
Tri, α	SSH	384	443	513	7	- 183	3
	GFRD	381	434	512	7	- 186	0

Goodness of fits are based on Akaike's information criterion (AIC) for maximum likelihood. Bold type indicates the best supported pigment and template scenarios based on AIC values

Mono = monochromatic template, Di = dichromatic template, Tri = trichromatic, α = scenarios where only alpha bands were considered, S, L and B = the modeled position of β -band(s) on short, long, or both pigments, respectively, λ_{max} = estimated wavelength (in nm) of maximum absorbance, p = number of parameters in a model

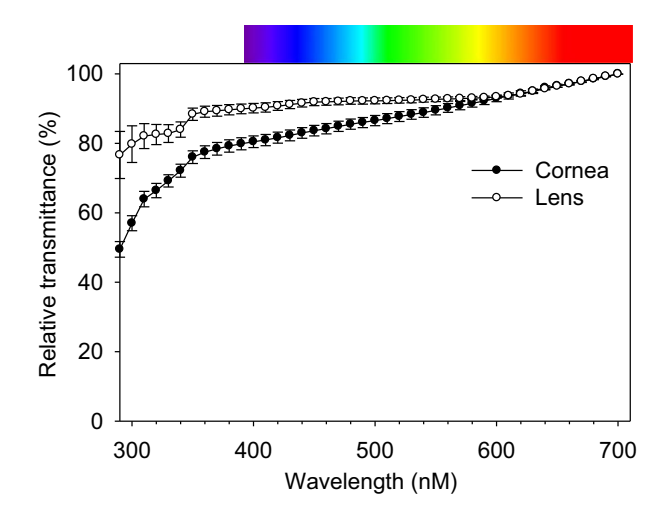


Fig. 5 Transmittance of lionfish ocular media at specific wavelengths. Data points (filled circles) are mean values (\pm SEM). The color bar indicates the approximate human visible spectrum

importantly, hypoxia reduced median scope for activity over all test temperatures, by 45, 48, 77, and 41 mg $O_2 kg^{-1} h^{-1}$ or by 71, 64, 69, and 41% at 15, 20, 25 and 30 °C, respectively (Fig. 7).

Critical oxygen levels

The S_{crit} of lionfish increased with every 5 °C increase in temperature and the relationship was linear (Fig. 8, panel a):

$$S_{crit} = (1.43 \pm 0.05 \times EC) + 10.6 \pm 1.3$$

 $r^2 = 0.99.$ (4)

To make our results directly comparable to those from other studies, we also express our data in units of oxygen concentration ($C_{\rm crit}$) (although this unit does not account for the effects of temperature and salinity on oxygen content at full saturation). The $C_{\rm crit}$ of lionfish increased over 10 °C increases in temperature (i.e., between 15 and 25 °C and between 20 and 30 °C) and the relationship was linear (Fig. 8, panel b):

$$C_{\text{crit}} = (0.049 \pm 0.002 \times \text{EC}) + 1.81 \pm 0.05$$

 $r^2 = 0.99.$ (5)

For comparative purposes, we have added S_{crit} and C_{crit} data for mid-Atlantic estuarine species (error bars are omitted for clarity): spot (*Leiostomus xanthurus*), croaker (*Micropogonias undulatus*) (Marcek et al. 2019), striped bass (Lapointe et al. 2014), and summer flounder (*Paralichthys dentatus*) (Capossela et al.



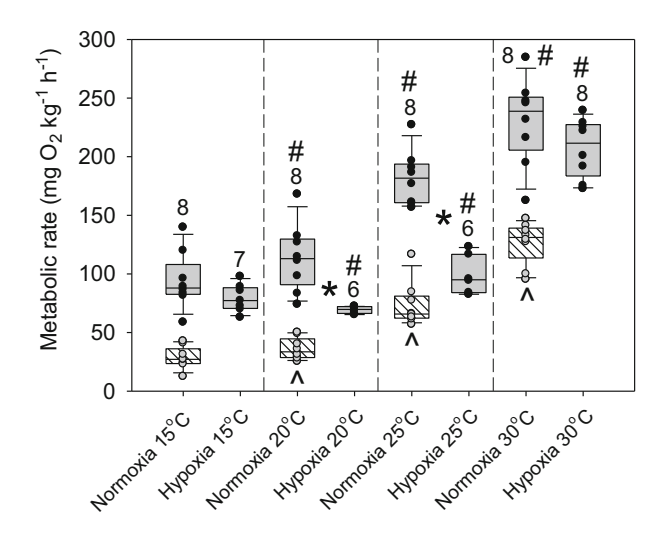


Fig. 6 Standard metabolic rates (SMR, cross-hatched bars and grey circles) in normoxia at three temperatures and active metabolic rates (AMR, grey bars and black circles) in normoxia at three temperatures. The symbols "^" and "#" indicate significant differences of SMR and AMR (respectively) between sequential temperature steps. The "*" symbol indicates significant differences in AMR in normoxia and hypoxia within test temperature. The boundary of the box closest to zero indicates the 25th percentile, the line within the box marks the median, and the boundary of the box farthest from zero indicates the 75th percentile. Whiskers (error bars) above and below the box indicate the 90th and 10th percentiles, respectively. Data points above and below the 90th and 10th percentiles are considered outliers. Numerical values signify the number of individuals tested

2012; Schwieterman et al. 2019). Both the $S_{\rm crit}$ and $C_{\rm crit}$ values for lionfish are above those of the other estuarine fishes at all temperatures, indicating that lionfish are less hypoxia tolerant.

Discussion

Functional characteristics of the visual system

We specifically chose to compare data on the functional characteristics of the visual system of lionfish to those of striped bass, bluefish, cobia, and summer flounder for the following reasons:

- data were collected using the same equipment, calibration methods, and data acquisition and analysis procedures,
- the life stages of the four native estuarine species were those which commonly occupy estuarine environments such as the Chesapeake Bay (e.g.,

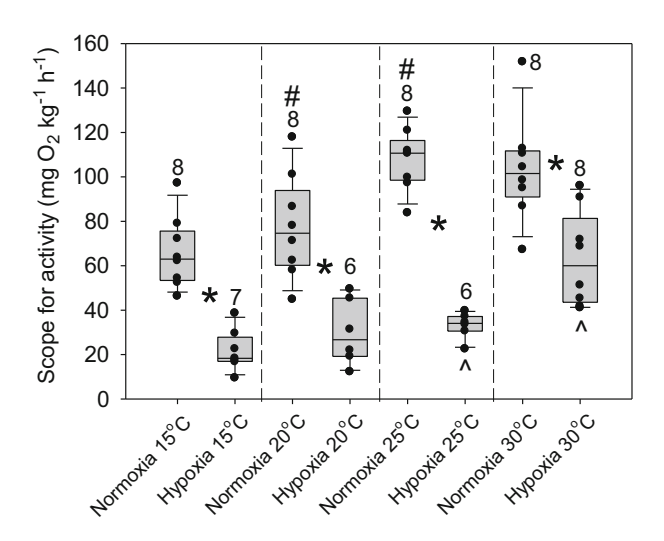


Fig. 7 Aerobic scope lionfish at various temperatures in normoxia and hypoxia (i.e., oxygen concentration 15-20% above $C_{\rm crit}$) conditions. The symbols "^" and "#" indicate significant differences in aerobic scope in hypoxia and normoxia (respectively) between sequential temperature steps. The "*" symbol indicates significant differences in aerobic scope in normoxia and hypoxia within test temperature. The boundary of the box closest to zero indicates the 25th percentile, the line within the box marks the median, and the boundary of the box farthest from zero indicates the 75th percentile. Whiskers (error bars) above and below the box indicate the 90th and 10th percentiles, respectively. Data points above and below the 90th and 10th percentiles are considered outliers. Numerical values signify the number of individuals tested

Buchheister et al. 2013; Buchheister and Latour 2015), and

3. the four native estuarine species are piscivores.

We therefore validated direct comparisons of data from lionfish and estuarine species through conservation of methods and the physiological mechanisms being investigated.

The K₅₀ of the lionfish visual system is approximately one log unit below that of three of the four estuarine piscivores (the exception being summer flounder, Fig. 2) implying that the lionfish visual system is functional at low light levels. Although lionfish are native to the clear tropical waters of the Indo-Pacific, they are crepuscular foragers in their native range (Green et al. 2019). In the western Atlantic, lionfish frequently occupy depths below 30 m and hunt more often on cloudy days (Morris and Akins 2009; Côté and Maljković 2010); situations where light levels are dim (McFarland and Loew 1983; Loew and McFarland 1990; Muntz 1990; Horodysky et al. 2010, 2013). Our results are,



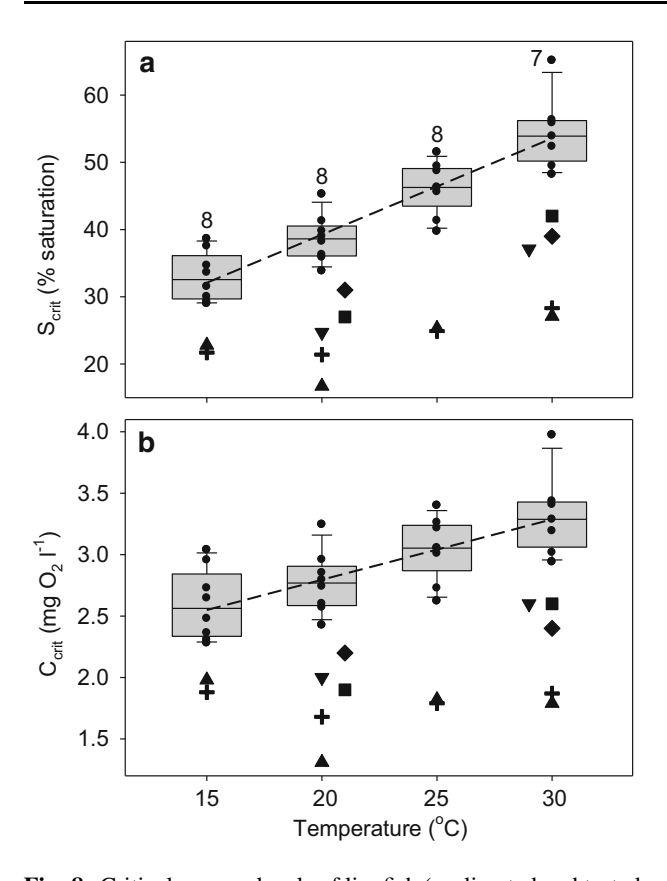


Fig. 8 Critical oxygen levels of lionfish (acclimated and tested at 15, 20, 25 and 30 °C) expressed as % air saturation (S_{crit}, a) or oxygen content (C_{crit} in mg $O_2 l^{-1}$, **b**). Mean C_{crit} values (error bars are omitted for clarity) of representative temperate estuarine species: cross = spot (*Leiostomus xanthurus*), triangle up = croaker (Micropogonias undulatus) (Marcek et al. 2019), triangle down = striped bass (Morone saxatilis) (Lapointe et al. 2014), diamond = summer flounder (*Paralichthys dentatus*) (Capossela et al. 2012), square = summer flounder (Schwieterman et al. 2019). The boundary of the box closest to zero indicates the 25th percentile, the line within the box marks the median, and the boundary of the box farthest from zero indicates the 75th percentile. Whiskers (error bars) above and below the box indicate the 90th and 10th percentiles, respectively. Data points above and below the 90th and 10th percentiles are considered outliers. Numerical values signify the number of individuals tested

therefore, congruent with lionfish visual ecology. More important, we conclude that the luminous sensitivity of the lionfish visual system is unlikely to preclude them from being effective piscivores estuarine environments. Indeed, their high sensitivity to dim light (i.e., low K_{50}) may enable lionfish to hunt successfully through most of the daylight hours in estuarine environments.

In contrast to luminous sensitivity, the dynamic range of the lionfish visual system is like that of three

of the other four estuarine piscivores (the exception being summer flounder, Fig. 2). The latter is a benthic ambush predator (Collette and Klein-MacPhee 2002) that most likely locates its prey by silhouetting them against downwelling light or the sand-water interface. Lionfish presumably sight prey horizontally (Morris and Akins 2009) as do striped bass, bluefish, and cobia. We conclude therefore that the dynamic range of the lionfish visual system is unlikely to preclude them from being effective piscivores in estuarine environments.

Flicker fusion frequency

Lionfish FFF at I₂₅ was not different from other estuarine piscivores, whereas lionfish FFF at I_{max} was \approx 33% higher than three of the four native estuarine piscivores (the exception being striped bass, Fig. 3). We presume that the high FFF of lionfish at I_{max} permits tracking fast-moving prey through structurally complex coral reef ecosystems in bright sunlight. As mentioned previously, however, lionfish are crepuscular foragers in their native range (Green et al. 2019). McComb et al. (2013) investigated FFF values of the piscivorous common snook (Centropomus undecimalis) and mangrove snapper (Lutjanus griseus) captured in the Indian River Lagoon (on the Atlantic coast of Florida, USA). The FFF of both (40 and 47 Hz, respectively) are within the 25–75% interval of FFF values of lionfish at I_{25} (32–45 Hz, Fig. 3). Although the lionfish median FFF at I_{max} is approximately double (88 Hz), we presume the former is more indicative of the performance of the lionfish visual system in generally light-limited estuarine environments. Because the FFF of lionfish at I₂₅ is equivalent to those of the other estuarine piscivores species at I_{25} (Fig. 3), we conclude that the FFF of the lionfish visual system is unlikely to preclude them from being effective predators under estuarine light conditions.

Spectral sensitivity

The spectral sensitivity of the lionfish visual system spans 350–620 nm, with the highest sensitivity at 510 nm (blue-green color wavelengths, Fig. 4). The relative transmittance of both the cornea and lens of lionfish (Fig. 5) supports our conclusions as to which wavelengths lionfish visual pigments are sensitive. It



is also congruent with ocular media transmission of coral reef fishes that have UV vision (Siebeck and Marshall 2001; Losey et al. 2003).

Rhodopsin templates fitted to ERG data predict that lionfish have three retinal pigments (i.e., are trichromats), with the short wavelength pigment absorbing in the near UV (Table 1). These results do not, however, preclude the alternate hypothesis that lionfish have only two visual pigments (i.e., are dichromats), but with a β-band on either visual pigment that absorbs in the near UV (Table 1). Furthermore, both Govardovskii and Stavenga rhodopsin templates generally exhibit fairly poor performance below 440 nm (Horodysky et al. 2008). Estuarine fishes are predominately dichromats, with maximum absorbances of short-wavelength pigments ranging from 440 to 460 nm and the maximum absorbances of longerwavelength pigments ranging 520-540 nm (e.g., Lythgoe and Partridge 1991; Jokela-Määttä et al. 2007; Horodysky et al. 2008, 2010). Dichromat rhodopsin templates fitted to lionfish ERG data estimate the maximum absorbance short-wave pigment of the visual pigment to be 460 nm, and the maximum absorbance of the long-wave pigment to be 513 nm (Table 1). These findings are congruent with the spectral sensitivity of mangrove snapper with two visual pigments (at 485 and 528 nm) whose visual system is maximally sensitive to blue-green wavelengths (McComb et al. 2013). If lionfish are dichromats, their spectral sensitivity would therefore be like those of native estuarine piscivores. Whether dicromats or trichromats, lionfish spectral sensitivity still overlaps the spectral composition of downwelling light in estuaries (570-700 nm at midday and 490-520 nm at twilight, Forward et al. 1988). We therefore conclude that the spectral sensitivity of lionfish visual system is unlikely to preclude them from being as effective piscivores under estuarine light conditions.

The question as to whether lionfish are dichromats or trichromats, and whether their apparent sensitivity to UV light arises from visual pigments residing in separate cone cells or is due to a β -band on other visual pigments, could be addressed using microspectrophotometry (e.g., Flamarique and Hárosi 2000; Mosk et al. 2007). We encourage investigations in this area. If present, the function of UV sensitivity residing in a separate cone cell is unclear. It is unlikely to be used for prey detection, as the life stage of lionfish

employed in our studies are piscivorous, not planktivorous. The latter employ UV sensitivity to improve contrast between their zooplankton prey and the surrounding veiling space light (Bowmaker 1990; Bowmaker and Kunz 1987). It is possible that lionfish are reflective in the UV, as are other tropical reef species, which would enhance their recognition of conspecifics (e.g., Losey et al. 1999, Marshall et al. 2015). We likewise encourage investigations in this area but recognize that our suggested efforts are not necessarily related to the ability of lionfish for estuarine invasion.

SMR, AMR, and scope for activity

We recognize the importance of studying the effects of temperature variability on metabolic performance in addition to temperature acclimation (Norin et al. 2014). The former was, however, beyond the resources available for our project. We likewise recognize that the chase protocol we used to estimate AMR may produce lower metabolic rate values than those measured at maximum sustainable speeds (Roche et al. 2013; Norin and Clark 2016). We presumed, however, that the latter methodology would be impractical with lionfish because of their large pectoral fins and sluggish hunting strategy. Steell et al. (2019) have, moreover, recently demonstrated that the metabolic rate of lionfish following feeding exceeds that following exhaustive exercise, reflecting the difficulties of defining maximum metabolic rate.

We likewise recognize that estimates of SMR can reflect methodological differences (Chabot et al. 2016). The median SMR we determined at 25 °C is similar to the mean SMR of lionfish at 26 °C reported by Steell et al. (2019), but well below that measured by Cerino et al. (2013) (Table 2). At 15, 20 and 25 °C, the SMR of lionfish is generally less than half those of representative species that occupy (at least seasonally) western mid-Atlantic estuaries, excluding flatfishes (Table 2). In contrast, at 30 °C the SMR of the species listed are roughly equivalent, apart from spot whose SMR is approximately double. The SMR of tropical scorpionfishes (Family Scorpaenidae; Scorpaenopsis oxycephalus, S. diabolus and Parascorpaena aurita; body mass 50 g) at 25 °C is 41 mg $O_2 \text{ kg}^{-1} \text{ h}^{-1}$ (Zimmermann and Kunzmann 2001) which is less than one-half of the median SMR of lionfish and, of course, well below SMR for representative temperate



Table 2 Metabolic rates (mg O_2 kg $^{-1}$ h $^{-1}$) of lionfish and representative mid-Atlantic estuarine fishes. For simplicity, we have omitted error terms and grouped data measured following exhaustive exercise, recorded during maximum sustainable swimming speeds, or the highest metabolic rates measured

under any condition under a single column. We made no corrections to account for the effects of body mass on weight-specific metabolic rates, as the necessary allometric scaling relationships are not available for all species

Species	15 °C		20 °C		25 °C		30 °C	
	SMR	AMR	SMR	AMR	SMR	AMR	SMR	AMR
Lionfish	27	88	34	113	66	161	131	239
Lionfish ^a	43		51		101		118	
Lionfish ^b					56	216*	81	206*
Lionfish ^b						320#		356#
Spot ^c	70-125	208	135–153	300	150-213	416-1275	242	528
Croaker ^d	52-74	152	70–89	202	102-124	310-869	137	367
Summer flounder ^e			45 (22 °C)				93	
Winter flounder ^f	43		77					

^aCerino et al. (2015

estuarine species. The low SMR of lionfish, other scorpaenids, and flatfishes could reflect their ambush-style foraging strategies. A low SMR would be advantageous as energy expenditure would be minimal when individuals are inactive.

In normoxia, the SMR of lionfish displayed a higher temperature sensitivity ($Q_{10} = 3.8$ and 4.0 between 20–25 °C and 25–30 °C, respectively) then the AMR $(Q_{10} = 2.6 \text{ and } 1.7 \text{ between } 20-25 \text{ °C and } 25-30 \text{ °C},$ respectively). This may be due to a decrease in efficacy of the cardiorespiratory system, such it can no longer supply oxygen and metabolic substrates to the tissues at high rates at the higher temperatures (Pörtner et al. 2017). The resultant plateau in scope for activity above 25 °C (Fig. 7) is likely to have implications with respect to fitness and performance during occupancy of shallow areas of mid-Atlantic estuaries where temperatures can exceed 30 °C (Rummer et al. 2014; Farrell 2016; Norin and Clark 2016; Baumann and Smith 2018). These observations do not imply, however, that elevated temperatures are likely to be a barrier to lionfish occupancy of mid-Atlantic estuaries. The plateau in lionfish scope for activity between 25 and 30 °C suggests an optimal

temperature range above 25 °C (Pörtner et al. 2017). Our observations are, therefore, in rough agreement with those of Barker et al. (2017) and Cerino et al. (2013) who found the final temperature preference of lionfish with gradual acclimation to be 29 ± 1 °C, and the optimal temperature for prey consumption to be 30 °C.

Overall, our results show that the effects of temperature on lionfish scope for activity can be divided into two stanzas: a plateau between 15 and 20 °C and a higher plateau between 25 and 30 °C (Fig. 7). The former suggests that lionfish could perform less frequent bouts of burst swimming (as these would necessitate quick recovery periods) and less frequent feeding bouts when prey items are abundant (because rates of digestion and protein assimilation are reduced) at temperatures between 15 and 20 °C than at temperatures between 25 and 30 °C. Both are dependent on a high scope for activity (Brill 1996; Claireaux et al. 2000; Claireaux and Lefrançois 2007; Clark et al. 2013; Steell et al. 2019). Our results on lionfish scope for activity do not, however, provide a mechanistic explanation for the reported cessation of feeding at 16 °C (Kimball et al. 2004), nor why the



^bSteell et al. (2019) (measurement temperatures, 26 and 32 °C; *after exhaustive exercise, *after feeding)

^cLeiostomus xanthurus (Horodysky et al. 2011; Marcek et al. 2019)

^dMicropogonias undulatus (Horodysky et al. 2011; Marcek et al. 2019)

^eParalichthys dentatus (Capossela et al. 2012)

^fPseudopleuronectes americanus (Cech et al. 1977)

geographic boundary for lionfish appears to be set by a minimum winter temperature of 15 °C (Whitfield et al. 2014), as scope for activity did not approach zero at these temperatures.

Hypoxia reduced both AMR (Fig. 6) and scope for activity (Fig. 7), although the relative effects of hypoxia on scope for activity occurred over every 5 °C increment in temperature and were relatively larger. More specifically, the fractional reductions in AMR under hypoxia were 47 and 11% at 20 and 25 °C, respectively; whereas the fractional reductions in scope of activity under hypoxia were 71, 64, 69, and 41% at 15, 20, 25 and 30 °C, respectively. The influence of temperature on the smaller reduction of scope for activity under hypoxia suggests that the optimal temperature range for lionfish under hypoxia is close to their final temperature preference under normoxia. In sum, we conclude that occupation of hypoxic areas will negatively impact lionfish, although the impact of hypoxia may be lower at water temperatures close to their final temperature preference (Barker et al. 2017). We recognize, however, that the relationship of temperature, hypoxia, SMR, AMR, and scope for activity is complex and nonlinear (e.g., Claireaux et al. 2000) and therefore warrants a more systematic exploration.

Scrit and Ccrit

Not surprisingly, lionfish resemble other teleost fishes in that they are oxygen regulators, possessing the physiological mechanisms necessary to maintain a constant metabolic rate until reaching their critical oxygen level (Schurmann and Steffensen 1997; Richards 2009; Ultsch and Regan 2019). We originally hypothesized that lionfish would be relatively intolerant of hypoxia because they evolved in the welloxygenated waters of the Indo-Pacific, and because the founder populations of lionfish in the western Atlantic came from there (Whitfield et al. 2002; Semmens et al. 2004). More specifically, we posited that episodic hypoxia common in estuaries (e.g. Breitburg 1992; Rabalais et al. 2010; Baumann and Smith 2018) would create a mismatch between environmental conditions and lionfish physiological capabilities that would limit their spread into these ecologically important inshore areas. Our results on critical oxygen levels support our hypothesis. The hypoxia tolerance of lionfish (measured as C_{crit}) is approximately half that of representative native estuarine fishes from western mid-Atlantic at all test temperatures (Fig. 8). The effects of temperature on lionfish hypoxia tolerance is less clear however. When hypoxia tolerance is expressed as C_{crit} (Fig. 8), 5 °C increases in temperature (i.e., 15-25 °C and 25-30 °C) do not affect hypoxia tolerance, whereas when comparing results over 10 °C temperature increases (i.e., 15-25 °C and 20-30 °C), C_{crit} values increase by almost 50% (i.e., hypoxia tolerance starkly declines). In contrast, a 5 °C temperature increase results in an average 18% increase in S_{crit} over all temperature intervals. The relationship of both S_{crit} and C_{crit} to temperature is linear ($r^2 = 0.99$) however, so either unit of measurement could be employed (using Eqs. 4 or 5) to predict the effects of hypoxia on lionfish distribution.

Given the intolerance of lionfish to hypoxia relative to native estuarine fishes, we conclude that hypoxic zones occurring in mid-Atlantic and Gulf of Mexico estuaries (oxygen saturation $\approx 25-40\%$; oxygen content $\approx 2-3 \text{ mg O}_2 \text{ l}^{-1}$; Baumann and Smith 2018) will constrain lionfish movements. We also conclude that lionfish will be limited to occupancy of the mouths of estuaries, or to shallow areas where oxygen levels remain above 50% saturation (Breitburg et al. 2003). For example, Eby and Crowder (2002) and Eby et al. (2005) have documented habitat compression due to seasonal hypoxia for native fishes and we predict that this will be more acute in lionfish. The extent and duration of seasonal hypoxia may also expand due to increases in agricultural runoff and urbanization that contributes to eutrophication, and the effects of directional climate change (e.g., Kemp et al. 2005; Robbins and Lisle 2018; Baumann and Smith 2018). It is unlikely, however, that lionfish will be subjected to the "temperature-oxygen squeeze" that forces striped bass to occupy warmer shallow waters outside their normal thermal range (i.e., < 25 °C; Coutant 1985; Martino and Secor 2009) during the summer months because deeper cooler waters (such as the mainstem of the Chesapeake Bay) are hypoxic (i.e., oxygen concentrations > 4 mg O_2 l^{-1}) (Breitburg 1992; Kemp et al. 2005). This supposition is based our observations of the effects of temperature on SMR, AMR and scope for activity, and the fact that the preferred and the physiologically optimal temperature for lionfish is 29 °C (Barker et al. 2017). We also recognize that episodic acidification (due to elevated dioxide levels) and hypoxia



simultaneously within estuaries (Baumann et al. 2015; Baumann and Smith 2018) and that these conditions have interactive effects on the metabolic rates, hypoxia tolerance, and sensory biology of fishes (e.g., Esbaugh 2018; Baumann 2019; Rivest et al. 2019; Schwieterman et al. 2019). Quantification of the combined effects of elevated CO₂ and temperature on metabolic and sensory physiology of lionfish was beyond the resources available for our project, but we encourage investigations in these areas.

Conclusion

Our intention was to quantify the physiological abilities of lionfish and thus to define environmental conditions that could limit their invasion into estuaries. The functional properties of the lionfish visual system appear similar enough to those of native piscivores that we infer they would not preclude lionfish occupation of Atlantic and Gulf of Mexico estuaries. Lionfish are, however, relatively intolerant of hypoxia (i.e., minimum survivable oxygen levels are higher than those native estuarine species) and hypoxia dramatically reduces lionfish scope of activity. We contend that episodic hypoxic areas, common in estuaries during the summer and fall months, will control or limit the invasion of lionfish into these ecosystems.

Acknowledgements This work was supported by the Rock the Ocean Foundation and Allen Levan. AZH was supported by NSF 1600691 and NSF 1846004. Special thanks to Dynasty Marine Associates Inc. in assisting with lionfish collections, Megan Byer who assisted with eye dissections, and Brian Naff who provided invaluable fish husbandry experience. This is contribution number 3882 from the Virginia Institute of Marine Science, College of William & Mary.

References

- Albins MA, Hixon MA (2008) Invasive Indo-Pacific lionfish *Pterois volitans* reduce recruitment of Atlantic coral-reef fishes. Mar Ecol Prog Ser 367:233–238
- Albins MA, Hixon MA (2013) Worst case scenario: potential long-term effects of invasive predatory lionfish (*Pterois volitans*) on Atlantic and Caribbean coral-reef communities. Environ Biol Fish 96:1151–1157
- Ali MA, Muntz WR (1975) Electroretinography as a tool for studying fish vision. Vision in fishes. Plenum Press, New York, pp 159–167

- Barbour AB, Montgomery ML, Adamson AA, Diaz-Ferguson E, Silliman BR (2010) Mangrove use by the invasive lionfish *Pterois volitans*. Mar Ecol Prog Ser 401:291–294
- Barker BD, Horodysky AZ, Kerstetter DW (2017) Hot or not? Comparative behavioral thermoregulation, critical temperature regimes, and thermal tolerances of the invasive lionfish *Pterois* sp. versus native western North Atlantic reef fishes. Biol Invasions 20:45–58
- Baumann H (2019) Experimental assessments of marine species sensitivities to ocean acidification and co-stressors: how far have we come? Can J Zool. https://doi.org/10.1139/cjz-2018-0198
- Baumann H, Smith EM (2018) Quantifying metabolically driven pH and oxygen fluctuations in US nearshore habitats at diel to interannual time scales. Estuaries Coasts 41:1102–1117
- Baumann H, Wallace R, Tagliaferri T, Gobler CJ (2015) Large natural pH, CO_2 and O_2 fluctuations in a temperate tidal salt marsh on diel, seasonal and interannual time scales. Estuaries Coasts 38:220–231
- Beck MW, Heck KL Jr, Able KW, Childers DL, Eggleston DB, Gillander BM, Halpern B, Hays CG, Hoshino K, Minello TJ, Orth RJ, Sheridan PF, Weinstein MP (2001) The identification, conservation, and management of estuarine and marine nurseries for fish and invertebrates. Bioscience 51:633–641
- Bernal NA, DeAngelis DL, Schofield PJ, Sealey KS (2015) Predicting spatial and temporal distribution of Indo-Pacific lionfish (*Pterois volitans*) in Biscayne Bay through habitat suitability modeling. Biol Invasions 17:1603–1614
- Bishop MJ, Powers PS, Porter HJ, Peterson CH (2006) Benthic biological effects of seasonal hypoxia in a eutrophic estuary predate rapid coastal development. Estuar Coast Shelf Sci 70:415–422
- Bowmaker JK (1990) Visual pigments of fishes. In: Douglas RH, Djamgoz MBA (eds) The visual system of fishes. Chapman & Hall, London, pp 63–81
- Bowmaker JK, Kunz YW (1987) Ultraviolet receptors, tetrachromatic colour vision and retinal mosaics in the brown trout (*Salmo trutta*): age dependent changes. Vis Res 27:2101–2108
- Breitburg DL (1992) Episodic hypoxia in Chesapeake Bay: interacting effects of recruitment, behavior, and physical disturbance. Ecol Monogr 62:525–546
- Breitburg DL, Adamack A, Rose KA, Kolesar SE, Decker B, Purcell JE, Keister JE, Cowan JH (2003) The pattern and influence of low dissolved oxygen in the Patuxent River, a seasonally hypoxic estuary. Estuaries 26:280–297
- Brill RW (1996) Selective advantages conferred by the higher performance physiology of tunas, billfishes, and dolphin fish. Comp Biochem Physiol 113A:3–15
- Brill R, Magel C, Davis M, Hannah R, Rankin P (2008) Effects of rapid decompression and exposure to bright light on visual function in black rockfish (*Sebastes melanops*) and Pacific halibut (*Hippoglossus stenolepis*). Fish Bull 106:427–437
- Browman HI (2005) Applications of sensory biology in marine ecology and aquaculture. Mar Ecol Prog Ser 287:266–269
- Brown KT (1968) The electroretinogram: its components and their origins. Vis Res 8:633–677



- Buchheister A, Latour RJ (2015) Diets and trophic-guild structure of a diverse fish assemblage in Chesapeake Bay, U.S.A.. J Fish Biol 86:967–992
- Buchheister A, Bonzek CF, Gartland J, Latour RJ (2013) Patterns and drivers of the demersal fish community of Chesapeake Bay. Mar Ecol Prog Ser 481:161–180
- Capossela KM, Brill RW, Fabrizio MC, Bushnell PG (2012) Metabolic and cardiorespiratory responses of summer flounder *Paralicthys dentatus* to hypoxia at two temperatures. J Fish Biol 81:1043–1058
- Carroll MR (2018) Spectral sensitivity of the invasive lionfish (*Pterois* species) retina and its capacity for change in response to lighting condition. MS thesis, Florida Institute of Technology
- Cech JJ, Rowell DW, Glasgow JS (1977) Cardiovascular responses of the winter flounder *Pseudopleuronectes* americanus to hypoxia. Comp Biochem Physiol 57A:123–125
- Cerino D, Overton AS, Rice JA, Morris JA Jr (2013) Bioenergetics and trophic impacts of the invasive Indo-Pacific lionfish. Trans Am Fish Soc 142:1522–1534
- Chabot D, Steffensen JF, Farrell AP (2016) The determination of standard metabolic rate in fishes. J Fish Biol 88:81–121
- Claireaux G, Chabot D (2016) Responses by fishes to environmental hypoxia: integration through Fry's concept of aerobic metabolic scope. J Fish Biol 88:232–251
- Claireaux G, Lefrançois C (2007) Linking environmental variability and fish performance: integration through the concept of scope for activity. Philos Trans R Soc B 362:2031–2041
- Claireaux G, Webber DM, Lagardère JP, Kerr SR (2000) Influence of water temperature and oxygenation on the aerobic metabolic scope of Atlantic cod *Gadus morhua*. J Sea Res 44:257–265
- Clark TD, Sandblom E, Jutfelt F (2013) Aerobic scope measurements of fishes in an era of climate change: respirometry, relevance and recommendations. J Exp Biol 216:2771–2782
- Coates MM, Garm A, Theobald JC, Thompson SH, Nilsson D-E (2006) The spectral sensitivity of the lens eyes of a box jellyfish, *Tripedalia cystophora* (Conant). J Exp Biol 209:3758–3765
- Collette BB, Klein-MacPhee G (2002) Bigelow and Schroeder's fishes of the Gulf of Maine, 3rd edn. Smithsonian Institution Press, Washington
- Cooke SJ, O'Connor CM (2010) Making conservation physiology relevant to policy makers and conservation practitioners. Conserv Lett 2:159–166
- Cooke SJ, Suski CD (2008) Ecological restoration and physiology: an overdue integration. Bioscience 58:957–968
- Cooke SJ, Sack L, Franklin CE, Farrell AP, Beardall J, Wikelski M, Chown SL (2013) What is conservation physiology? Perspectives on an increasingly integrated and essential science. Conserv Physiol. https://doi.org/10.1093/conphys/cot/001
- Côté IM, Green SJ (2012) Potential effects of climate change on a marine invasion: the importance of current context. Curr Zool 58:1–8
- Côté IM, Maljković A (2010) Predation rates of Indo-Pacific lionfish on Bahamian coral reefs. Mar Ecol Prog Ser 404:219–225

- Côté IM, Smith NS (2018) The lionfish *Pterois* sp. invasion: has the worst-case scenario come to pass? J Fish Biol 92:660–689
- Côté IM, Green SJ, Hixon MA (2013) Predatory fish invaders: insights from Indo-Pacific lionfish in the western Atlantic and Caribbean. Biol Conserv 164:50–61
- Courrat A, Lobry J, Nicolas D, Laffargue P, Amara R, Lepage M, Girardin M, Le Pape O (2009) Anthropogenic disturbance on nursery function of estuarine areas for marine species. Estuar Coast Shelf Sci 81:179–190
- Courtenay WR (1995) Marine fish introductions in southeastern Florida. Am Fish Soc Introd Fish Sect Newsl 1995:2–3
- Coutant CC (1985) Striped bass, temperature, and dissolved oxygen: a speculative hypothesis for environmental risk. Trans Am Fish Soc 114:31–61
- Dabruzzi TF, Bennett WA, Fangue NA (2017) Thermal ecology of red lionfish *Pterois volitans* from southeast Sulawesi, Indonesia, with comparisons to other Scorpaenidae. Aquat Biol 26:1–14
- Dangles O, Irschick D, Chittka L, Casas J (2009) Variability in sensory ecology: expanding the bridge between physiology and evolutionary biology. Q Rev Biol 84:51–74
- Diaz RJ (2001) Overview of hypoxia around the world. J Environ Qual 30:275–281
- Diaz RJ, Breitburg DL (2009) The hypoxic environment. In: Richards JG, Farrell AP, Brauner CJ (eds) Fish physiology, vol 27. Academic Press, San Diego, pp 1–23
- Douglas R, Djamgoz M (1990) The visual system of fish. Chapman and Hall, London
- Eby LA, Crowder LB (2002) Hypoxia-based habitat compression in the Neuse River Estuary: context-dependent shifts in behavioral avoidance thresholds. Can J Fish Aquat Sci 59:952–965
- Eby LA, Crowder LB, McClellan CM, Peterson CH, Powers MJ (2005) Habitat degradation from intermittent hypoxia: impacts on demersal fishes. Mar Ecol Prog Ser 291:249–261
- Esbaugh AJ (2018) Physiological implications of ocean acidification for marine fish: emerging patterns and new insights. J Comp Physiol B 188:1–13
- Farrell AP (2016) Pragmatic perspective on aerobic scope: peaking, plummeting, pejus and apportioning. J Fish Biol 88:322–343
- Ferreira CEL, Luiz OJ, Floeter SR, Lucena MB, Barbosa MC, Rocha CR, Rocha LA (2015) First record of invasive lionfish (*Pterois volitans*) for the Brazilian coast. PLoS ONE 10:e0123002
- Fishelson L (1997) Experiments and observations on food consumption, growth, and starvation in *Dendrochirus brachypterus* and *Pterois volitans* (Pteroinae, Scorpaenidae). Environ Biol Fish 50:391–403
- Flamarique IN, Hárosi FI (2000) Photoreceptors, visual pigments, and ellipsosomes in the killifish, *Fundulus heteroclitus*: a microspectrophotometric and histological study. Vis Neurosci 17:403–420
- Forward RB Jr, Cronin TW, Douglass JK (1988) The visual pigments of crabs II. Environmental adaptations. J Comp Physiol 162:479–490
- Frank TM (2003) Effects of light adaptation on the temporal resolution of deep-sea crustaceans. Integr Comp Biol 43:559–570



- Fritsches KA, Brill RW, Warrant EJ (2005) Warm eyes provide superior vision in swordfishes. Curr Biol 15:55–58
- Fry FEJ (1947) Effect of the environment on animal activity. Univ Toronto Stud Biol Ser 55:1–62
- Fry FEJ (1971) The effect of environmental factors on the physiology of fish. In: Hoar WS, Randall DJ (eds) Fish physiology, vol 6. Academic Press, New York, pp 1–98
- Fry FEJ, Hart JS (1948) The relation of temperature to oxygen consumption in the goldfish. Biol Bull 94:66–77
- Gallegos CL, Jordan TE, Hines AH, Weller DE (2005) Temporal variability of optical properties in a shallow, eutrophic estuary: seasonal and interannual variability. Estuar Coast Shelf Sci 64:156–170
- González J, Grijalba-Bendeck M, Acero A, Betancur R (2009) The invasive red lionfish, *Pterois volitans* (Linnaeus 1758), in the southwestern Caribbean Sea. Aquat Invasions 4:507–510
- Govardovskii VI, Fyhrquist N, Reuter T, Kuzmin DG, Donner K (2000) In search of the visual pigment template. Vis Neurosci 17:509–528
- Green SS, Akins LJ, Côté IM (2011) Foraging behavior and prey consumption in the Indo-Pacific lionfish on Bahamian coral reefs. Mar Ecol Prog Ser 433:159–167
- Green SJ, Akins JL, Maljković A, Côté IM (2012) Invasive lionfish drive Atlantic coral reef fish declines. PLoS ONE 7:e32596
- Green SJ, Dilley ER, Benkwitt CE, Davis ACD, Ingeman KE, Kindinger TL, Tuttle LJ, Hixon MA (2019) Trait-mediated foraging drives patterns of selective predation by native and invasive coral-reef fishes. Ecosphere 10:e02752. https://doi.org/10.1002/ecs2.2752
- Guthrie DM, Muntz WRA (1993) Role of vision in fish behavior. In: Pitcher TJ (ed) Behavior of teleost fishes, 2nd edn. Chapman and Hall, London, pp 89–128
- Hixon MA, Green SJ, Albins MA, Akins JL, Morris JA Jr (2016) Lionfish: a major marine invasion. Mar Ecol Prog Ser 558:161–165
- Horodysky AZ, Brill RW, Warrant EJ, Musick JA, Latour RJ (2008) Comparative visual function in five sciaenid fishes inhabiting Chesapeake Bay. J Exp Biol 211:3601–3612
- Horodysky AZ, Brill RW, Warrant EJ, Musick JA, Latour RJ (2010) Comparative visual function in four piscivorous fishes inhabiting Chesapeake Bay. J Exp Biol 213:1751–1761
- Horodysky AZ, Brill RW, Bushnell PG, Musick JA, Latour RJ (2011) Comparative metabolic rates of common western North Atlantic Ocean sciaenid fishes. J Fish Biol 79:235–255
- Horodysky AZ, Brill RW, Crawford KC, Seagroves ES, Johnson AK (2013) Comparative visual ecophysiology of mid-Atlantic temperate reef fishes. Biol Open 2:1371–1381
- Horodysky AZ, Cooke SJ, Brill RW (2015) Physiology in the service of fisheries science: why thinking mechanistically matters. Rev Fish Biol Fisher 25:425–447
- Ingeman KE (2016) Lionfish cause increased mortality rates and drive local extirpation of native prey. Mar Ecol Prog Ser 558:235–245
- Jud ZR, Layman CA, Lee JA, Arrington DA (2011) Recent invasion of a Florida (USA) estuarine system by lionfish *Pterois volitans/P. miles*. Aquat Biol 13:21–26

- Jud ZR, Nichols PK, Layman CA (2014) Broad salinity tolerance in the invasive lionfish *Pterois* spp. may facilitate estuarine colonization. Environ Biol Fish 98:135–143
- Kalinoski M, Hirons A, Horodysky A, Brill R (2014) Spectral sensitivity, luminous sensitivity, and temporal resolution in three sympatric temperate coastal shark species. J Comp Physiol B 200:997–1013
- Kemp WM, Boynton WR, Adolf JE, Boesch DF, Boicourt WC,
 Brush G, Cornwell JC, Fisher TR, Gilbert PM, Hagy JD,
 Harding LW, Houde ED, Kimmell DG, Miller WD, Newell
 RIE, Roman MR, Smith EM, Stevenson JC (2005)
 Eutrophication of the Chesapeake Bay: historical trends
 and ecological interactions. Mar Ecol Prog Ser 303:1–29
- Kimball ME, Miller JM, Whitfield PE, Hare JA (2004) Thermal tolerance and potential distribution of invasive lionfish (*Pterois volitans/miles* complex) on the east coast of the United States. Mar Ecol Prog Ser 283:269–278
- Ladich F, Collin SP, Moller P, Kapoor BG (2006) Communication in fishes, vol 2. Science Publisher, Enfield
- Lapointe D, Vogelbein WK, Fabrizio MC, Gauthier DT, Brill RW (2014) Temperature, hypoxia, and mycobacteriosis: effects on adult striped bass *Marone saxatilis* metabolic performance. Dis Aquat Organ 108:113–127
- Lennox R, Choi K, Harrison PM, Paterson JE, Peat TP, Ward TD, Cooke SJ (2015) Improving science-based invasive species management with physiological knowledge, concepts, and tools. Biol Invasions 17:2213–2227
- Loew ER, McFarland WN (1990) The underwater visual environment. In: Douglas R, Djamgoz M (eds) The visual system of fish. Chapman and Hall, London, pp 1–44
- Losey GS, Cronin TW, Goldsmith TH, Hyde D, Marshall NJ, McFarland WN (1999) The UV visual world of fishes: a review. J Fish Biol 54:921–943
- Losey GS, Mcfarland WM, Loew ER, Zamzow JP, Nelson PA, Marshall NJ (2003) Visual biology of Hawaiian coral reef fishes. I. Ocular transmission and visual pigments. Copeia 2003:433–454
- Lythgoe JN (1979) Ecology of vision. Clarendon Press, Oxford Lythgoe JN (1988) Light and vision in the aquatic environment.

 In: Atema J, Fay RR, Popper AN, Tavolga WN (eds) Sensory biology of aquatic animals. Springer, New York, pp 131–149
- Lythgoe JN, Partridge JC (1991) The modelling of optimal visual pigments of dichromatic teleosts in green coastal waters. Vis Res 31:361–371
- Marcek BJ, Brill RW, Fabrizio MC (2019) Metabolic scope and hypoxia tolerance of Atlantic croaker (*Micropogonias undulatus* Linnaeus, 1766) and spot (*Leiostomus xanthurus* Lacepède, 1802), with insights into the effects of acute temperature change. J Exp Mar Biol Ecol 516:150–158
- Marras S, Cucco A, Antognarelli F, Azzurro A, Milazzo M, Bariche M, Butenschön M, Kay S, Di Bitetto M, Quattrocchi G, Sinerchia M, Domenici P (2015) Predicting future thermal habitat suitability of competing native and invasive fish species: from metabolic scope to oceanographic modelling. Conserv Physiol. https://doi.org/10.1093/conphys/cou059
- Marshall J, Carleton KL, Cronin T (2015) Colour vision in marine organisms. Curr Opin Neurobiol 34:86–94
- Martino E, Secor D (2009) Warming and climate change. In: Striped Bass Species Team background and issue briefs.



- Ecosystem based fisheries management for Chesapeake Bay. Publ no. UM-SG-TS-2009-07, Maryland Sea Grant, College Park, MD
- McComb DM, Kajiura SM, Horodysky AZ, Frank TM (2013) Comparative visual function in predatory fishes from the Indian River Lagoon. Physiol Biochem Zool 86:285–297
- McCormick MI, Allan BJM (2016) Lionfish misidentification circumvents an optimized escape response by prey. Conserv Physiol 4:cow064. https://doi.org/10.1093/conphys/cow064
- McFarland WN, Loew ER (1983) Wave produced changes in underwater light and their relations to vision. Environ Biol Fish 8:173–184
- McKenzie DJ, Axelsson M, Chabot D, Claireaux G, Cooke SJ, Corner RA, De Boeck G, Domenici P, Guerreiro PM, Hamer B, Jørgensen C, Killen SS, Lefevre S, Marras S, Michaelidis B, Nilsson GE, Peck MA, Perez-Ruzafa A, Rijnsdorp AD, Shiels HA, Steffensen JF, Svendsen JC, Svendsen MBS, Teal LR, Van der Meer J, Wang T, Wilson JM, Wilson RW, Metcalfe JD (2016) Conservation physiology of marine fishes: state of the art and prospects for policy. Conserv Physiol 4:1–20
- Morris JA (2012) Invasive lionfish: a guide to control and management. Gulf and Caribbean Fisheries Institute special publication series number 1, Marathon, Florida
- Morris JA, Akins JL (2009) Feeding ecology of invasive lionfish (*Pterois volitans*) in the Bahamian archipelago. Environ Biol Fish 86:389. https://doi.org/10.1007/s10641-009-9538-8
- Mosk V, Thomas N, Hart NS, Partridge JC, Beazley LD, Shand J (2007) Spectral sensitivities of the seahorses *Hippocampus* subelongatus and *Hippocampus* barbouri and the pipefish Stigmatopora argus. Vis Neurosci 24:345–354
- Muntz WRA (1990) Stimulus, environment and vision in fishes. In: Douglas R, Djamgoz M (eds) The visual system of fish. Chapman and Hall, London, pp 419–511
- Munz FW, McFarland WN (1973) The significance of spectral position in the rhodopsins of tropical marine fishes. Vis Res 13:1829–1874
- Norin T, Clark TD (2016) Measurement and relevance of maximum metabolic rate in fishes. J Fish Biol 88:122–151
- Norin T, Malte H, Clark TD (2014) Aerobic scope does not predict the performance of a tropical eurythermal fish at elevated temperatures. J Exp Biol 217:244–251
- Parkyn DC, Hawryshyn CW (2000) Spectral and ultravioletpolarization sensitivity in juvenile salmonids: a comparative analysis using electrophysiology. J Exp Biol 203:1173–1191
- Pörtner H-O, Bock C, Mark FC (2017) Oxygen- and capacitylimited thermal tolerance: bridging ecology and physiology. J Exp Biol 220:2685–2696. https://doi.org/10.1242/ jeb.134585
- Prosser CL (1973) Temperature. In: Prosser CL (ed) Comparative animal physiology. WB Saunders, Philadelphia, pp 362–428
- Rabalais NN, Diaz RJ, Levin LA, Turner RE, Gilbert D, Zhang J (2010) Dynamics and distribution of natural and human-caused hypoxia. Biogeosciences 7:585–619
- Richards FA (1965) Dissolved gases other than carbon dioxide. In: Riley JP, Skirrow G (eds) Chemical oceanography. Academic Press, New York

- Richards JG (2009) Metabolic and molecular responses of fish to hypoxia. In: Richards JG, Farrell AP, Brauner CJ (eds) Fish physiology: hypoxia, vol 27. Elsevier, San Diego, pp 443–485
- Rivest EB, Jellison B, Ng G, Satterthwaite EV, Bradley HL, Williams SL, Gaylord B (2019) Mechanisms involving sensory pathway steps inform impacts of global climate change on ecological processes. Front Mar Sci. https://doi.org/10.3389/fmars.2019.00346
- Robbins LL, Lisle JT (2018) Regional acidification trends in Florida shellfish estuaries: a 20+ year look at pH, oxygen, temperature, and salinity. Estuar Coasts 41:1268–1281
- Roche DG, Binning SA, Bosiger Y, Johansen JL, Rummer JL (2013) Finding the best estimates of metabolic rates in a coral reef fish. J Exp Biol 216:2103–2110
- Rogers NJ, Urbina MA, Reardon EE, McKenzie DJ, Wilson RW (2016) A new analysis of hypoxia tolerance in fishes using a database of critical oxygen level (P_{crit}). Conserv Physiol 4:cow012. https://doi.org/10.1093/conphys/cow012
- Rummer JL, Couturier CS, Stecyk JAW, Gardiner NM, Kinch JP, Nilsson GE, Munday PL (2014) Life on the edge: thermal optima for aerobic scope of equatorial reef fishes are close to current day temperatures. Glob Change Biol 20:1055–1066
- Sandblom E, Gräns A, Axelsson M, Seth H (2014) Temperature acclimation rate of aerobic scope and feeding metabolism in fishes: implications in a thermally extreme future. Proc R Soc B 281:20141490. https://doi.org/10.1098/rspb.2014. 1490
- Saszik S, Bilotta J (1999) The effects of temperature on the darkadapted spectral sensitivity function of the adult zebrafish. Vis Res 39:1051–1058
- Schubert H, Sagert S, Forster RM (2001) Evaluation of the different levels of variability in the underwater light field of a shallow estuary. Helgol Mar Res 55:12–22
- Schurmann H, Steffensen JF (1997) Effects of temperature, hypoxia and activity on the metabolism of juvenile Atlantic cod. J Fish Biol 50:1166–1180
- Schwieterman GD, Crear DP, Anderson BN, Lavoie DR, Sulikowski JA, Bushnell PG (2019) Brill RW (2019) Combined effects of acute temperature change and elevated pCO₂ on the metabolic rates and hypoxia tolerances of clearnose skate (*Rostaraja eglanteria*), summer flounder (*Paralichthys dentatus*), and thorny skate (*Amblyraja radiata*). Biology 8:56. https://doi.org/10.3390/biology8030056
- Semmens BX, Buhle ER, Salomon AK, Pattengill-Semmens CV (2004) A hotspot of non-native marine fishes: evidence for the aquarium trade as an invasion pathway. Mar Ecol Prog Ser 266:239–244
- Siebeck UE, Marshall JN (2001) Ocular media transmission of coral reef fish—can coral reef fish see ultraviolet light? Vis Res 41:133–149
- Snyder S, Nadler LE, Bayley JS, Svendsen MBS, Johansen JL, Domenici P, Steffensen JF (2016) Effect of closed v. intermittent-flow respirometry on hypoxia tolerance in the shiner perch *Cymatogaster aggregata*. J Fish Biol 88:252–264
- Stavenga DG, Smiths RP, Hoenders BJ (1993) Simple exponential functions describing the absorbance bands of visual pigment spectra. Vis Res 33:1011–1017



- Steell SC, Van Leeuwen TE, Brownscombe JW, Cooke SJ, Eliason EJ (2019) An appetite for invasion: digestive physiology, thermal performance and food intake in lion-fish (*Pterois* spp.). J Exp Biol 222:jeb209437
- Steffensen JF (1989) Some errors in respirometry of aquatic breathers: how to avoid them and correct for them. Fish Physiol Biochem 6:49–59
- Svendsen MBS, Bushnell PG, Steffensen JF (2016) Design and setup of intermittent-flow respirometry system for aquatic organisms. J Fish Biol 88:26–50
- Tyler RM, Brady DC, Targett TE (2009) Temporal and spatial dynamics of diel-cycling hypoxia in estuarine tributaries. Estuaries Coasts 32:123–145
- Ultsch GR, Regan MD (2019) The utility and determination of P_{crit} in fishes. J Exp Biol 222:jeb203646
- Weissgerber TL, Milic NM, Winham SJ, Garovic VN (2015) Beyond bar and line graphs: time for a new data presentation paradigm. PLoS Biol 13:e1002128
- Whitfield PE, Gardner T, Vives SP, Gilligan MR, Courtenay WR, Ray GC, Hare JA (2002) Biological invasion of the

- Indo-Pacific lionfish *Pterois volitans* along the Atlantic coast of North America. Mar Ecol Prog Ser 235:289–297
- Whitfield PE, Muñoz RC, Buckel CA, Degan BP, Freshwater DW, Hare JA (2014) Native fish community structure and Indo-Pacific lionfish *Pterois volitans* densities along a depth-temperature gradient in Onslow Bay, North Carolina, USA. Mar Ecol Prog Ser 509:241–254
- Wing SR, Leichter JJ, Denny MW (1993) A dynamic model for wave induced light fluctuations in a kelp forest. Limnol Oceanogr 38:396–407
- Wood CM (2018) The fallacy of the P_{crit} —are there more useful alternatives? J Exp Biol 221:jeb163717
- Zimmermann C, Kunzmann A (2001) Baseline respiration and spontaneous activity of sluggish marine tropical fish of the family Scorpaenidae. Mar Ecol Prog Ser 219:229–239

Publisher's Note Springer Nature remains neutral with regard to jurisdictional claims in published maps and institutional affiliations.

